We are IntechOpen, the world's leading publisher of Open Access books Built by scientists, for scientists

6,900
Open access books available

186,000
International authors and editors

200M
Downloads

154
Countries delivered to

Our authors are among the

TOP 1%
most cited scientists

12.2%
Contributors from top 500 universities

CLARIVATE ANALYTICS
BOOK CITATION INDEX
INDEXED

WEB OF SCIENCE™

Selection of our books indexed in the Book Citation Index
in Web of Science™ Core Collection (BKCI)

Interested in publishing with us?
Contact book.department@intechopen.com

Numbers displayed above are based on latest data collected.
For more information visit www.intechopen.com

Synergetic Control of a Hybrid Battery-Ultracapacitor Energy Storage System

Rached Dhaouadi, Kamyar Khosravi and Yoichi Hori

Additional information is available at the end of the chapter

Abstract

This chapter presents a synergy-based cascade control scheme for a hybrid battery-ultracapacitor (UC) energy storage system. The purpose is to improve the dynamic response of the battery-based energy storage system using an ultracapacitor module as an auxiliary energy storage unit. A bidirectional DC-DC converter is designed to interface between the ultracapacitor module and the main DC-bus. The control scheme is based on a fast inner current control loop using sliding mode control and an outer loop for DC-bus voltage regulation using synergy-based control. The improvement in performance is demonstrated through simulation and experiments. The results show that the DC-bus voltage is well regulated under external load disturbances with fast dynamic transients. The ultracapacitor module is able to absorb the sudden load variations and limit the battery power requirements by maintaining an optimal power balance between the two embedded storage units. The performance of the proposed synergy-based controller is compared with the standard PI controller, and its ability to achieve optimal transient performance is verified.

Keywords: DC-DC converter, hybrid energy storage system, synergetic control, ultracapacitor

1. Introduction

The rapid development of the automotive industry has resulted in a variety of technological enhancements in electric vehicles (EV), which have significantly improved fuel consumption and reduced emissions. However, EV technology still faces many challenges such as long drive

range, long battery operating life, and high charge–discharge cycle rate in order to recover as much of the vehicle's kinetic energy as possible and supply high peak energies on demand [1–4].

For the EV operation, it is important to predict the battery energy demand for a specific trip. However, the stochastic driving cycles and unpredictable power demand may lead to a fast discharge action of batteries, resulting in an energy shortage to complete the given trip. A backup energy storage unit is therefore necessary to supply a stable and reliable power to the vehicle and improve the steady-state and dynamic behavior under different operating conditions [5, 6].

Ultracapacitors (UCs) are nowadays recognized as a viable auxiliary power source with outstanding power characteristics. They have been integrated successfully with energy storage systems for many industrial applications such as electric vehicles and photovoltaic energy systems [7–13]. The inclusion of UC can be very useful to maintain stability in electrical power systems with distributed generation by enhancing the output from lead-acid batteries and intermittent renewable resources.

In electric vehicles, the main power source is usually a lithium-ion battery, or a fuel cell, and the mechanical load is coupled to a permanent-magnet synchronous machine (PMSM) through an inverter. To extend the driving range of the vehicle and enable more efficient use of the batteries, a UC module is used as an auxiliary power source connected to the DC-bus through a bidirectional DC-DC converter. This configuration allows obtaining an optimized charge/discharge operation to smooth the power fluctuations and reinforce the DC-bus during the load transients [14–17].

During the last decade, different control techniques based on adaptive control theory, sliding mode control, fuzzy logic, and neural networks have been proposed for the control of DC-DC power converters [18, 19]. The main objective of such nonlinear controllers is to provide the control support for boost-type converters to improve their controllability and performance for large operating ranges.

Recently, the synergetic control appears to be a novel effective approach to deal with many nonlinear control problems due to its optimality property and its inherent robustness to disturbances. The synergetic control was developed by Kolesnikov et al. [20] on the basis of the standard variable structure control. The method was later applied to a number of industrial processes, including problems in energy conversion [21–25]. In [24], the authors presented the optimization characteristic of the synergetic control method and showed that the control law can be derived using the analytical design of aggregated regulators (ADAR) method and calculus of variation principles.

The main features of synergetic control are that it is well-suited for digital implementation; it gives constant switching frequency operation and gives better control of the off-manifold dynamics. Switching converters have intrinsic nonlinear and time-varying characteristics, which make the synergetic controller to also be a well-suited control scheme. The other important advantages of this control approach are order reduction, decoupling design procedure, and insensitivity to parameter variation.

This chapter presents a new control scheme to improve the dynamic response of a battery-based energy storage system using an UC module as an auxiliary energy storage unit. This chapter represents a preliminary study for EV applications. The primary objective is to improve both the vehicle range and the battery cycle life through optimal management of the onboard power and energy, and realize full utilization of the installed storage capacities.

The originality of the proposed technique is the procedure to develop the synergy-based cascade control scheme and to devise the link between the system variables to have an accurate control of the DC-bus voltage and an optimal management of the power flow between the battery, UC module, and load. Additionally, our contribution extends the analysis of the synergy-based cascade control scheme by providing a proof of the controller stability using Lyapunov theory.

A prototype hybrid battery/UC system is developed to perform experimental analysis and validate the proposed controller. Experimental results and a comparison with the standard PI controller are given to validate the optimal transient performance of the synergy-based controller.

The proposed synergy-based control scheme is shown to have the following characteristics:

- Synergetic control improves the dynamic response of the UC energy storage system.

- UC absorbs sudden load variations and limits battery power requirements.

- The control scheme maintains an optimal power balance between the storage units.

- Synergy-based control is robust to external load disturbances and UC voltage variation.

2. Hybrid energy storage system

Figure 1 shows the proposed topology used for electric vehicles. The system has a DC-coupled structure where a UC module is used as an auxiliary power source and connected to the
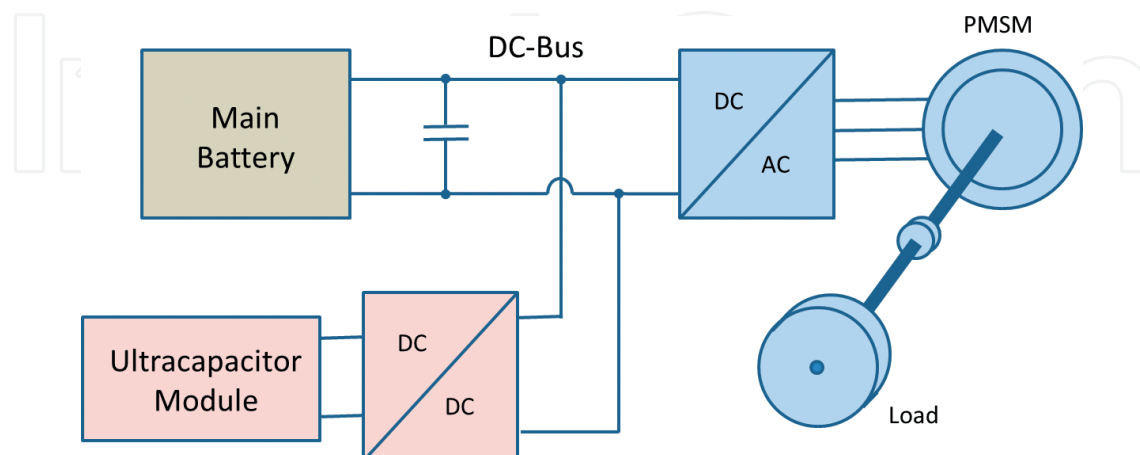
Figure 1. Topology of the hybrid energy storage system.

DC-bus through a bidirectional DC-DC converter. The proposed hybrid energy storage system is designed to have high efficiency and regenerative energy capture capability. These two features represent the key elements with respect to energy saving in electric vehicles. The battery is the main DC power source that forms the DC-bus. Various loads including the AC drive motors and auxiliary electrical loads are fed from the DC-bus through DC-AC and DC-DC converters. The AC drive motors represent the main load. A UC is interfaced to the DC-bus through a bidirectional DC-DC converter to control the energy transfer between the battery and the UC module. The power converter circuit consists of two MOSFET switches in a bridge configuration combined with an inductor and a capacitor as shown in **Figure 2**. The converter is connected to the UC module on the low-voltage side and to the lead-acid battery on the high-voltage side. The circuit is controlled through a PWM signal generated by the hysteresis current controller.

The power converter regulates the energy flow to and from the UC in two modes of operation: buck and boost, depending on the direction of the inductor current. The converter operates in the boost mode when energy is transferred from the UC to the battery.

On the other hand, the converter operates in the buck mode when energy is transferred from the battery to the UC, or if energy is recovered from the load (regenerative breaking). The power converter is assumed to operate in continuous conduction PWM mode while switching between two states depending on the status of the switches (Q_1, Q_2).

In the first PWM state, Q_1 is ON and Q_2 is OFF, while in the second PWM state, Q_1 is OFF and Q_2 is ON. In the boost mode of operation, the converter circuit is described by the following equations:

$$L\frac{di_L}{dt} = v_c - (R_s + R_L)i_L - v_0(1 - u), \tag{1}$$

$$C_f\frac{dv_0}{dt} = i_L(1 - u) - i_0 + i_b, \tag{2}$$

$$C_s\frac{dv_c}{dt} = -i_L, \tag{3}$$

where u is the average control factor of the switch Q_2, L is the inductance, C_s is the ultracapacitance, C_f is the filter capacitance, R_L is the internal inductor resistance, i_b is the battery current, i_L is the inductor current, i_0 is the load current, v_0 is the output voltage, v_c is the ultracapacitor voltage, and R_s is the internal resistance (ESR) of the ultracapacitor.

In the literature, different electro-circuit models for UC behavior simulation are available. These models have different degrees of complexity and simulation qualities [26–27]. In this chapter, the focus is on the validation of the synergy-based controller concept, the UC is modeled as a pure supercapacitance in series with the equivalent ESR. The measured UC voltage is given by:

$$\begin{aligned} v_s &= v_c + R_s i_{sc} \\ i_{sc} &= -i_L \end{aligned} \tag{4}$$

where i_{sc} is defined as the UC current. A positive i_{sc} means that the UC is charging, while a negative i_{sc} means that the UC is discharging.
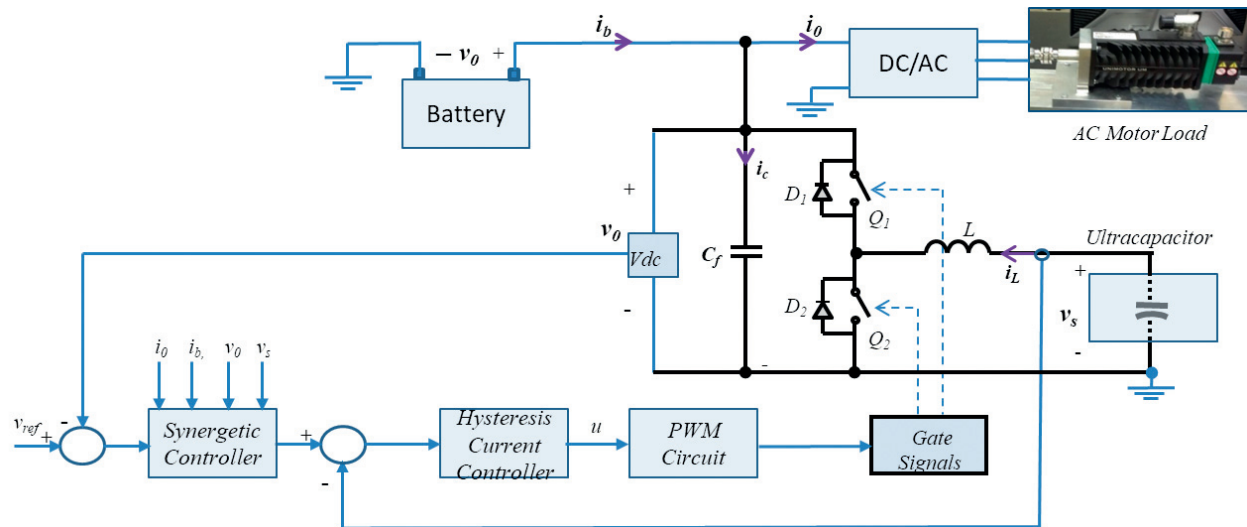
Figure 2. Block diagram of the proposed synergy-based hybrid energy storage system.

The battery is modeled by an equivalent RC circuit with a series–parallel branch as given by Eq. (5). C_b represents the charge storage capacity of the battery, R_b is the internal series resistance (ESR), and R_d is used to model the long-term storage performance of the battery [13].

$$C_b \frac{dv_b}{dt} + \frac{v_b}{R_d} + i_b = 0 .$$
$$v_0 = v_b - R_b i_b \tag{5}$$

The state space equations of the energy storage system can be obtained by taking i_L, v_0, v_c, and v_b as state variables, and considering the load current i_0 as the system input:

$$\frac{d}{dt}\begin{bmatrix} i_L \\ v_0 \\ v_c \\ v_b \end{bmatrix} = \begin{bmatrix} -\frac{(R_s + R_L)}{L} & -\frac{\bar{u}}{L} & \frac{1}{L} & 0 \\ \frac{\bar{u}}{C_f} & -\frac{1}{R_b C_f} & 0 & \frac{1}{R_b C_f} \\ -\frac{1}{C_s} & 0 & 0 & 0 \\ 0 & \frac{1}{R_b C_b} & 0 & -\frac{1}{C_b}\left(\frac{1}{R_b} + \frac{1}{R_d}\right) \end{bmatrix} \begin{bmatrix} i_L \\ v_0 \\ v_s \\ v_b \end{bmatrix} + \begin{bmatrix} 0 \\ -\frac{1}{C_f} \\ 0 \\ 0 \end{bmatrix} i_0, \tag{6}$$

where $\bar{u} = 1 - u$ is the switch control signal.

3. Cascade control scheme with sliding mode current control

The DC-bus voltage regulation is achieved by using a cascade control structure with a fast inner current control loop and an outer synergy-based voltage control loop. The current control loop is implemented using a sliding mode scheme to achieve a fast-response and robust performance. As a result, the inductor current is controlled to follow the reference

current I_r, within a given tolerance band, in order to charge or discharge the ultracapacitor and keep a regulated output DC-bus voltage v_0. The main objective is to keep the output voltage at the desired value even under external disturbances and load variations. **Figure 2** shows the overall control scheme of the energy management system.

First, a current switching line is defined

$$S(x) = I_r - i_L = 0, \tag{7}$$

where $I_r > 0$ is the reference current. Sliding motion exists in the region where $v_s < v_0$. The condition $\frac{dS}{dt} = 0$ is obtained by using Eq. (1):

$$\frac{v_0}{L}(1 - u) - \frac{v_s}{L} = 0. \tag{8}$$

The equivalent control is

$$0 < u_{eq} = 1 - \frac{v_s}{v_0} < 1. \tag{9}$$

The hysteresis current controller is a very high gain controller permitting the measured current to properly track the reference signal with high accuracy. Therefore, if the tolerance band is very small, the current control loop can be approximated by a unity block. Hence, the converter equations reduce to $i_L \approx I_r$ and $u = u_{eq}$.

In EV applications, a sudden acceleration or deceleration is equivalent to a step load torque change. Therefore, a variable load current can be used to represent the nonlinear DC-AC converter characteristics together with the AC motors.

The energy storage system model is next modified to include the load as a variable resistance R_0. The load current can then be expressed as: $i_0 = \frac{v_0}{R_0}$.

The resulting converter equations are nonlinear in terms of the output voltage v_0.

$$\begin{cases} \dfrac{dv_0}{dt} = -\dfrac{1}{C_f}\left(\dfrac{1}{R_b} + \dfrac{1}{R_0}\right)v_0 + \dfrac{1}{R_b C_f}v_b + \dfrac{1}{C_f}\left(\dfrac{v_s}{v_0}\right)I_r \\ \dfrac{dv_b}{dt} = \dfrac{1}{R_b C_b}v_0 - \dfrac{1}{C_b}\left(\dfrac{1}{R_b} + \dfrac{1}{R_d}\right)v_b \\ \dfrac{dv_c}{dt} = -\dfrac{1}{C_s}I_r \end{cases}. \tag{10}$$

The Lyapunov stability method is next used to analyze the voltage Eqs. (10). The output voltage equation is the main nonlinear equation and can be written in the following form:

$$\frac{dv_0}{dt} = \frac{a}{v_0} - bv_0 + d, \tag{11}$$

where $a = \frac{1}{C_f}I_r v_s$, $b = \frac{1}{R_0 C_f}$, and $d = \frac{1}{C_f}i_b$.

Next, a Lyapunov function is defined as

$$F = \frac{1}{2b}\left(v_0 - \sqrt{\frac{a}{b}}\right)^2.$$ (12)

Then

$$\dot{F} = \frac{1}{b}\left(v_0 - \sqrt{\frac{a}{b}}\right) \times \frac{dv_0}{dt} = \frac{1}{b}\left(v_0 - \sqrt{\frac{a}{b}}\right)\left(\frac{a}{v_0} - bv_0 + d\right),$$ (13)

which can be rewritten in the following form:

$$\dot{F} = -\frac{1}{v_0}\left(v_0 - \sqrt{\frac{a}{b}}\right)\left(v_0{}^2 - \frac{d}{b}v_0 - \frac{a}{b}\right) = -\frac{1}{v_0}\left(v_0 - \sqrt{\frac{a}{b}}\right)f(v_0).$$ (14)

The roots of the function $f(v_0) = 0$ are

$$\begin{cases} v_{01} = \frac{1}{2}\left(R_0 i_b - \sqrt{R_0{}^2 i_b^2 + 4R_0 I_r v_s}\right) \\ v_{02} = \frac{1}{2}\left(R_0 i_b + \sqrt{R_0{}^2 i_b^2 + 4R_0 I_r v_s}\right) \end{cases}.$$ (15)

The stability condition of the system Eq. (10) is guaranteed if $\dot{F} < 0$. This condition is satisfied if

$$v_0 > \frac{1}{2}\left(R_0 i_b + \sqrt{R_0{}^2 i_b^2 + 4R_0 I_r v_s}\right).$$ (16)

4. Synergetic control

The synergetic control scheme is next developed by analyzing the reduced system voltage equations with sliding mode current control as described by (10). The nonlinear system can be written in the following form:

$$\dot{x} = f(x, w, t),$$ (17)

where $x = [v_0 \ v_s]^t$ is the state vector, v_0 is the system output, and $w = I_r$ is the system input.

The objective is to devise a control law $I_r = f(v_0, v_s)$ that optimizes the required voltage regulation $v_0 = v_{0r}$ under different operating conditions.

Let $L(t, \sigma, \dot{\sigma})$ be a function with continuous first and second derivatives with respect to all of its arguments. The objective is to find the function $\sigma(x(t))$ that is continuously differentiable for $t_0 \leq t \leq t_f$ and satisfy boundary conditions $\sigma(t_0) = \sigma_0$ and $\sigma(t_f) = \sigma_f$, for which the functional

$$J = \int_{t_0}^{t_f} L(t, \sigma(t), \dot{\sigma}(t)) dt = \int_{t_0}^{t_f} \left(T^2 \dot{\sigma}^2 + \sigma^2 \right) dt, \tag{18}$$

is minimum, where $T = T^T > 0$ is a symmetric positive parameter to be designed. Then, $\sigma(t)$ is a minimizer of the functional J if it is a solution of the following linear differential equation

$$T\dot{\sigma} + \sigma = 0, \tag{19}$$

where T is a design parameter that sets the speed of convergence to the desired manifold.

Next, define the macro-variable σ as

$$\sigma = v_0 - v_{0r} + k_1(v_s - v_{sr}) + k_2 \int_0^t (v_0 - v_{0r}) dt. \tag{20}$$

The reference voltage v_{0r} can be selected to be the nominal DC-bus voltage with no load when the UC is in the charging mode. On the other hand, the reference voltage v_{sr} is selected as the rated voltage of the UC. Next, the macro-variable derivative is obtained using the chain rule of differentiation.

$$\dot{\sigma} = \frac{d\sigma}{dx} \dot{x}. \tag{21}$$

Using (18)–(21) and solving for the reference current I_r yields

$$I_r = \frac{1}{\frac{k_1}{C_s} - \frac{v_s}{C_f v_0}} \times \left[\frac{i_b - i_0}{C_f} + \left(k_2 + \frac{1}{T} \right)(v_0 - v_{0r}) + \frac{k_1}{T}(v_s - v_{sr}) + \frac{k_2}{T} \int (v_0 - v_{0r}) dt \right]. \tag{22}$$

This synergetic control law will force the system to operate on the manifold $\sigma(x) = 0$. In addition, the control law will impose a well-controlled dynamic behavior off the manifold.

Next, the control law designed earlier is shown to be globally asymptotically stable. Consider the positive definite candidate Lyapunov function V is defined by

$$V(x) = \frac{1}{2}\sigma^2(x). \tag{23}$$

Then, the total time derivative of V along the trajectories of $\sigma(x)$ is given by

$$\dot{V} = \sigma(x)\dot{\sigma}(x) = -\frac{1}{T}\sigma^2(x) < 0 \qquad \forall \sigma \neq 0, \tag{24}$$

which shows that the system (10) will converge to the manifold $\sigma(x) = 0$ asymptotically.

5. Optimized control law

The synergy-based control strategy presented earlier uses a cascade control structure where the output voltage is regulated by the outer loop via the inductor current which is tightly

controlled by a faster inner loop. This strategy is shown to give a good transient performance. However, it is very sensitive to the UC voltage v_s, since this voltage is continuously changing due to charging and discharging actions. To overcome this drawback, an optimized control law is adopted by filtering the UC voltage v_s to detect and use the low-frequency variation instead of the actual voltage.

The new manifold is then updated as

$$\Psi = v_0 - v_{0r} + k_1 v_{sf} + k_2 \int_0^t (v_0 - v_{0r}) dt, \tag{25}$$

where v_{sf} is the filtered UC voltage. A first order low-pass filter is used with a cut-off frequency ω_f and a transfer function

$$G_f(s) = \frac{\omega_f}{s + \omega_f}. \tag{26}$$

6. Simulation results

The proposed synergetic control law is validated first using computer simulation. The closed loop system behavior is evaluated by checking the system robustness to step load disturbances. The simulation results are next validated on an experimental prototype system with the same input parameters.

Figure 3 shows the system performance when starting at no load, and then the load current is changed from 0 to 2.6 A. It can be observed that initially the DC-bus voltage v_0 is stabilized at the desired reference value of 32.7 V. Next, due to the sudden variation in load, the voltage is disturbed and goes through a fast transient. The synergetic controller is able to minimize the
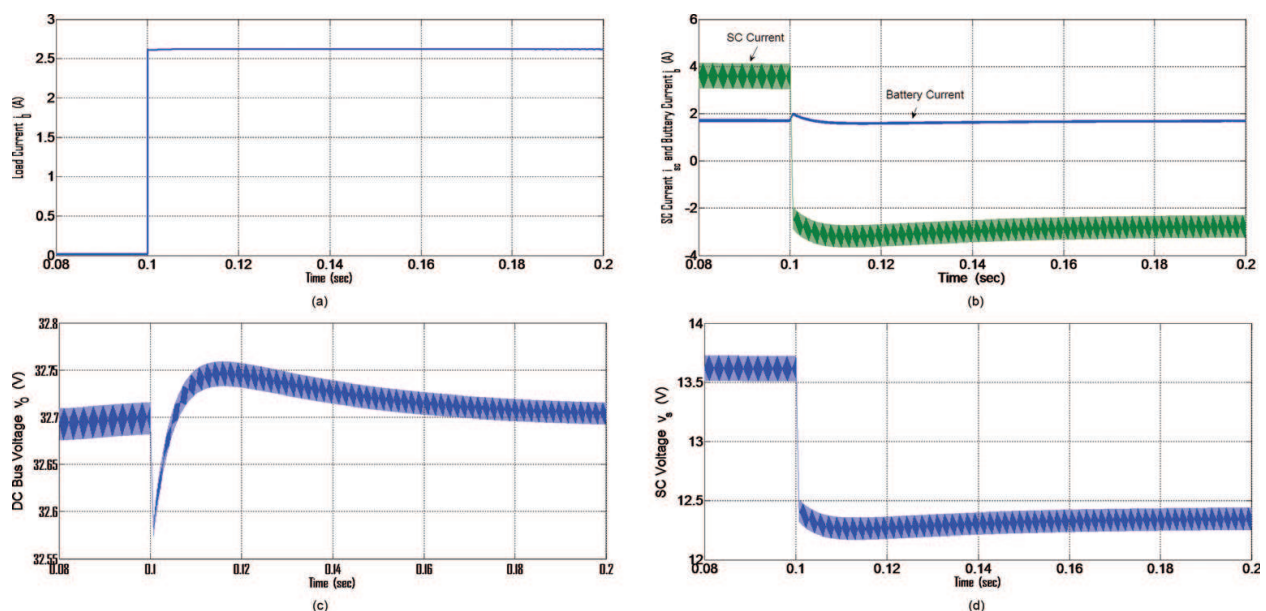
Figure 3. System response to a step load current with optimized control law. (**a**) Load current i_0; (**b**) DC-bus voltage v_0; (**c**) battery current i_b and SC current i_{sc}; and (**d**) SC voltage v_s.

voltage fluctuation, and the voltage is regulated back to the reference value. The peak-to-peak voltage variation is

$$\Delta v_0 = \frac{v_{0\mathrm{max}} - v_{0\mathrm{min}}}{v_{0r}} = 0.56\%. \tag{27}$$

The sudden load increase at $t = 0.1s$ is quickly supplied by the UC, which is discharged through the inductor. The battery shows only a small variation in current which contains only a low-frequency component needed for voltage regulation. This response is a good feature of the proposed control system that would help extend the battery operating life. The results clearly illustrate that the optimized control system has a very good robust performance to load uncertainty. The incorporation of the low-pass filter allows tracking the voltage changes with fast transient response and very small steady-state error.

7. Experimental results and discussion

In this section, experimental results of the proposed synergy-based control scheme are provided to validate the theoretical design. **Figure 4** shows a general view of the actual hardware. The synergetic controller block is implemented by Eq. (22) as illustrated in **Figure 2**. The system parameters are given in **Table 1**.

The hybrid energy storage system prototype was developed using a bidirectional DC-DC converter module, a 36-V battery pack, and a 15-V UC bank formed by the series connection of six UCs with 2300 F each. The variable load is implemented by using two 25 Ω power resistors in parallel connected to the DC-bus. The control algorithms are developed on the eZdsp board from Texas Instruments based on the TMS320F28335 DSP and the dSPACE1104 development system. The TI DSP is solely dedicated to the current control loop, while the dSPACE1104 system is for the outer voltage control loop. The control code is developed by the operator on a laptop using Code Composer Studio and then downloaded on the TI-DSP for real-time operation.

The closed loop system behavior is analyzed by evaluating the transient response and steady-state response to step load disturbances. The first test examines the case where the DC-bus voltage is maintained at a constant value with no load and the battery is charging only the UC with a constant current.

The DC-bus voltage reference is set to a value $v_{0r} = 32.85V$ lower than the nominal value of the battery. The synergetic controller would then automatically set the charging current reference for the UC to maintain this DC-bus voltage level. The load is next changed abruptly as shown in the profile of **Figure 5**. Normally, this would require an abrupt change of the battery current to supply this sudden load disturbance. However, the system shows a very good robustness to this load disturbance, as the UC current changes rapidly from the charging mode to the discharging mode to supply the required additional load with the minimum effect on the battery current.
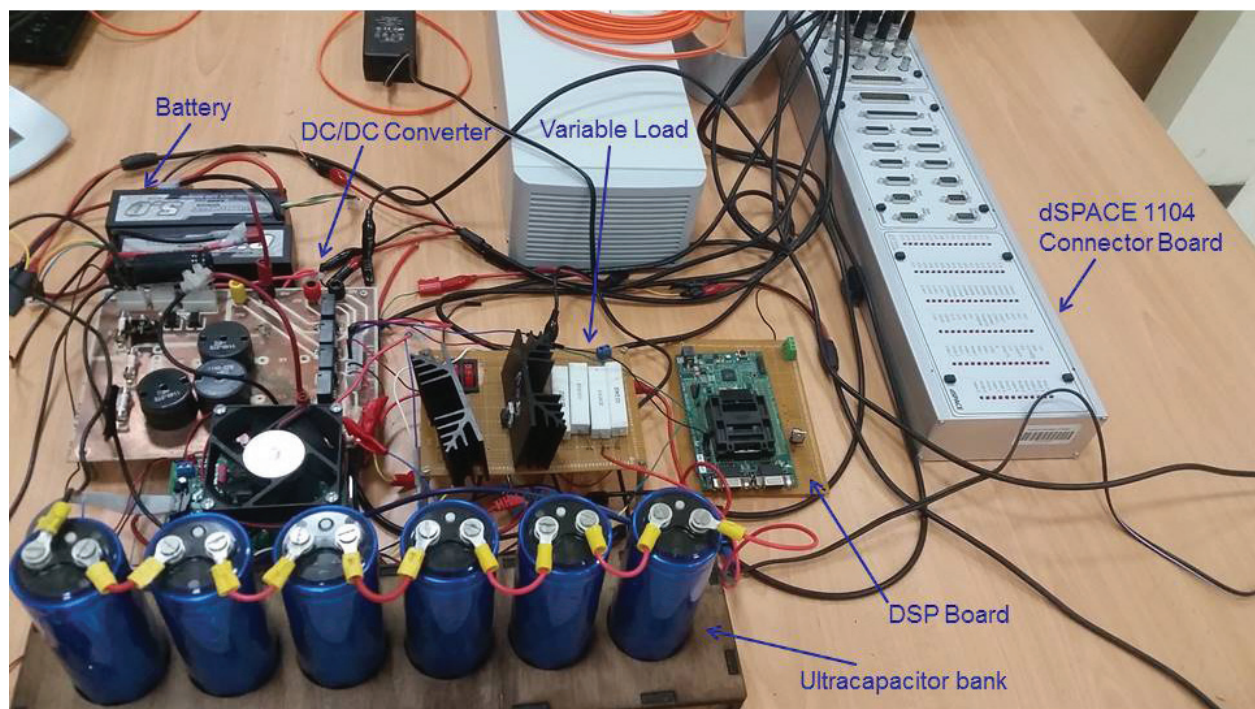
Figure 4. Hardware prototype of the proposed UC-based energy storage system.

Symbol	Parameter	Value
R_0	Resistive load	25 Ω
L	Inductance	1.35 H
R_L	Inductor Internal Resistance	0.2 Ω
C_s	UC Bank	383.3 F
R_s	UC Bank Internal Resistance	0.2 Ω
C_f	Output capacitor	4700 μF
v_{sn}	Nominal UC voltage	15 V
v_{bn}	Nominal battery voltage	42 V
C_b	Battery storage capacitor	900 F
R_b	Battery internal series resistance (ESR)	0.4 Ω
R_d	Battery storage resistance	470 Ω
T_s	Outer Loop Sampling time	12.5 μs
t_s	Current Control Loop Sampling Time	5 μs
Δi	Current controller Hysteresis band	0.5 A
T	Synergetic Controller Time Constant	10 ms
k_1	Synergetic Controller Gain	0.01
k_2	Synergetic Controller Gain	100

Table 1. Prototype system parameters.
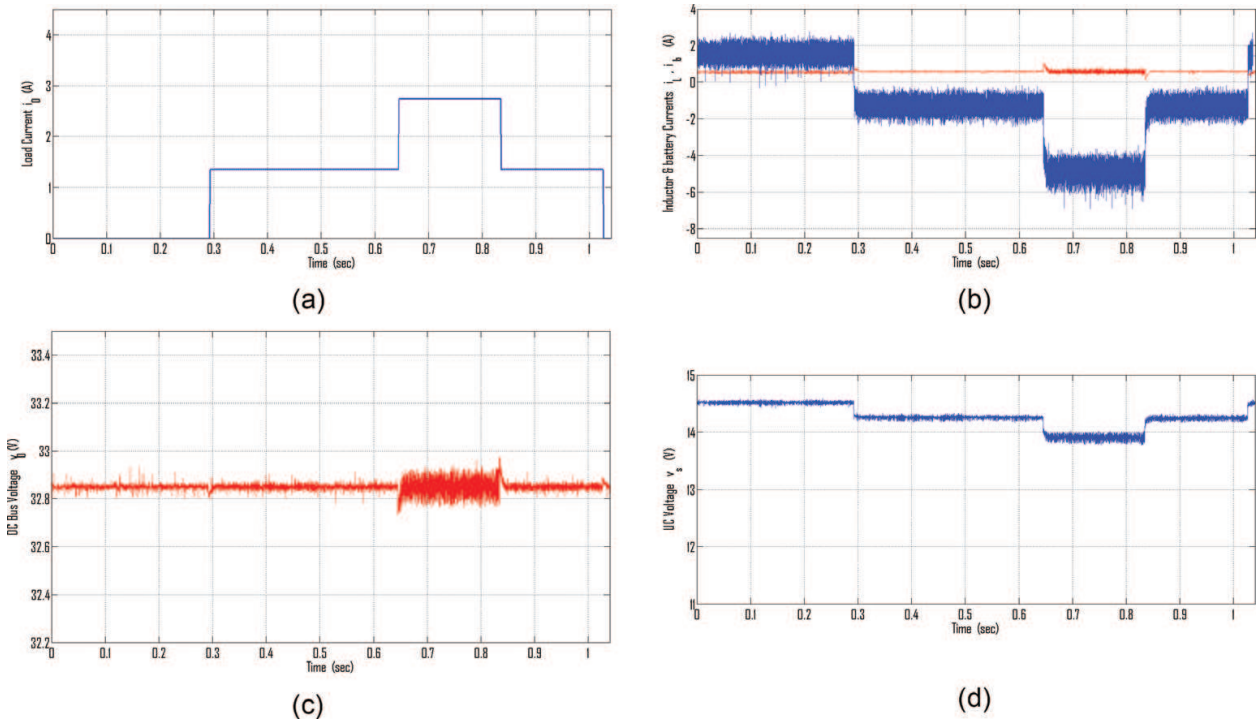
Figure 5. Experimental results with synergetic controller and variable load. (**a**) Load current i_0; (**b**) DC-bus voltage v_0; (**c**) battery current i_b and SC current i_{sc}; and (**d**) SC voltage v_s.

The output voltage also maintains its steady-state value with minimum variation, except at large load, when the ripple voltage is increased. This is mainly due to the large inductor current ripple. Despite the large variation in load, the peak-to-peak voltage variation is

$$\Delta v_0 = \frac{v_{0max} - v_{0min}}{v_{0r}} = \frac{32.97 - 32.76}{32.85} = 0.73\%. \tag{28}$$

This result shows a very good agreement with the simulation results obtained in Section 5.

The transient performance of the proposed synergetic controller is next compared with the standard PI controller, and its ability to achieve optimal transient performance is verified. The PI voltage control loop is implemented using the measured output DC-bus voltage.

$$I_r = k_p(v_{0r} - v_0) + k_i \int_0^t (v_{0r} - v_0)dt. \tag{29}$$

Figures 6 and **7** show the system response to a load step change for both controllers under the same operating conditions. The DC-bus voltage is regulated to follow a reference value $v_{0r} = 32.7V$. The PI controller gains were tuned to achieve a fast transient response while keeping the overshoot below 1%.

A step load change (i_0 = 2.56 A) is applied at t = 0.0047 s. For the PI controller, the DC-bus voltage is reduced due to this sudden load change as shown in **Figure 6b**. It goes through a transient and then recovers back to the reference value within 10.7 ms. For the synergetic

controller, the voltage deviation is smaller, and the transient response is faster with a settling time of 7.1 ms as shown in **Figure 7b**. The battery and supercapacitor currents' behavior can be compared by referring to **Figure 6c** and **Figure 7c**. In both cases, the UC current changes rapidly from the charging mode to the discharging mode to supply the required additional load current. However, it can be observed that the battery current shows a larger variation and
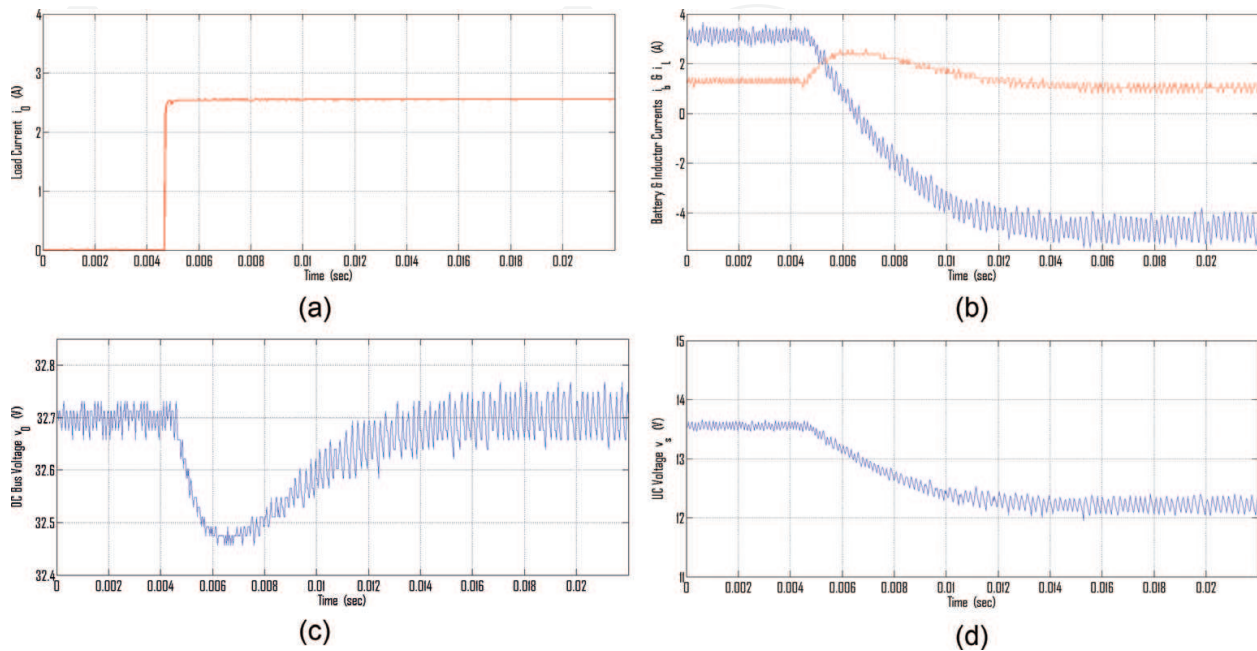
Figure 6. Experimental results with PI controller and a step load. (**a**) Load current ; (**b**) DC-bus voltage v_0; (**c**) battery current i_b and SC current i_{sc}; and (**d**) SC voltage v_s.
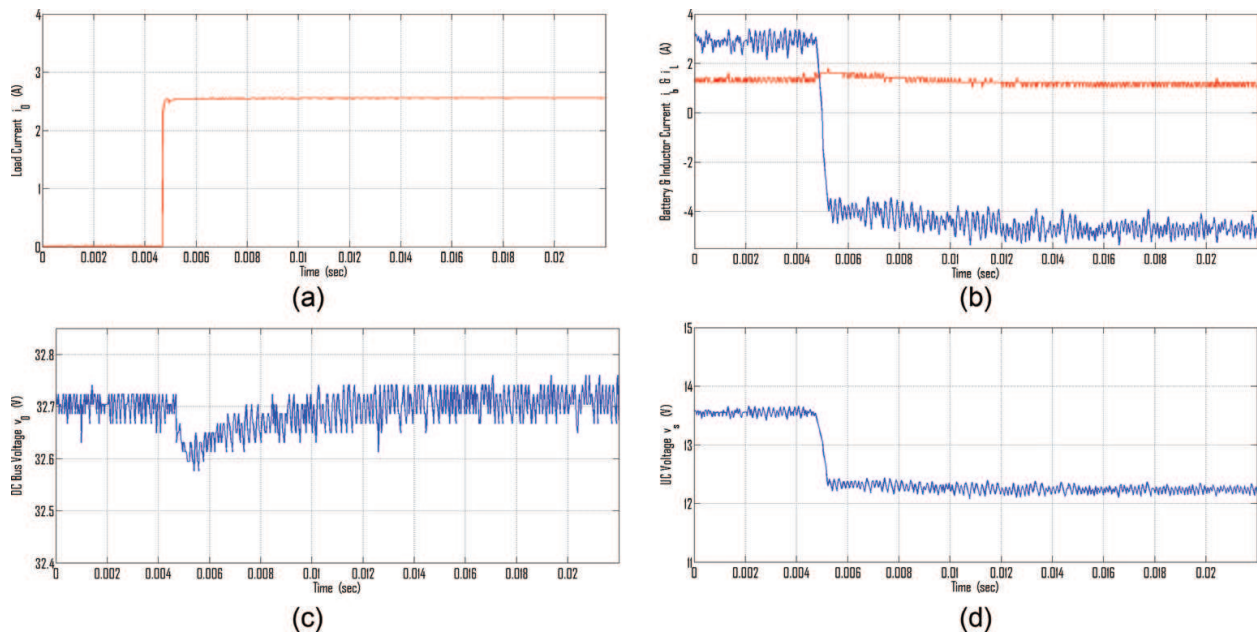
Figure 7. Experimental results with synergetic controller and a step load. (**a**) Load current i_0; (**b**) DC-bus voltage v_0; (**c**) battery current i_b and SC current i_{sc}; and (**d**) SC voltage v_s.

a slower response for the case of the PI controller compared to the synergetic controller. The same behavior is observed for the UC voltage in **Figure 6d** and **Figure 7d**.

Table 2 gives the peak-to-peak variations of the battery current and the DC-bus voltage for both controllers. It can be seen that the synergy-based controller has a much better transient performance and a higher robustness to disturbances than the PI controller.

Controller		PI controller	Synergetic controller
Battery current variation	$\Delta i_b = \frac{i_{b\max} - i_{b\min}}{i_{ss}}$	96.50%	37.13%
DC-bus voltage variation	$\Delta v_0 = \left| \frac{v_{0\max} - v_{0\min}}{v_{0r}} \right|$	0.73%	0.37%
Settling time	To reach steady state	10.7 ms	7.1 ms

Table 2. Experimental results with PI controller and synergetic controller under variable load.

8. Conclusion

This chapter proposes a fast-response synergetic controller for a battery-ultracapacitor energy storage system. The synergy-based controller is developed to enhance the system robustness during the transient response of the DC-bus voltage tracking control. The ultracapacitor module is controlled to reinforce the DC-bus during the load transients and smooth the power fluctuations. The stability analysis of the nonlinear control scheme is derived using the Lyapunov theory. The effectiveness of the proposed control scheme is verified by simulations and by experiments on a prototype hybrid energy storage system and its advantages are indicated in comparison with the traditional PI control scheme. This work is intended as a preliminary study to optimize the performance of electric vehicles. It is believed that the presented technique will provide a strong foundation for the development of a range of full-field synergy-based control techniques in electric vehicles. The added advantages of this technique is that it has a cascade control structure which can be easily adapted and implemented on existing EV control systems. Only additional current and voltage sensors are needed to implement the feedback control loops. This could be a versatile tool to improve both the vehicle range and battery cycle life through optimal management of the onboard power and energy and realize full utilization of the installed storage capacities.

Author details

Rached Dhaouadi[1]*, Kamyar Khosravi[1] and Yoichi Hori[2]

*Address all correspondence to: rdhaouadi@aus.edu

1 College of Engineering, American University of Sharjah, Sharjah, UAE

2 Graduate School of Frontier Science, The University of Tokyo, Chiba, Japan

References

[1] Dyke KJ, Schofield N, Barnes M. The impact of transport electrification on electrical networks. IEEE Transactions on Industrial Electronics. 2010;**57**(12):3917-3926

[2] Sant AV, Khadkikar V, Xiao W, Zeineldin HH. Four-Axis vector-controlled dual-rotor PMSM for plug-in electric vehicles. IEEE Transactions on Industrial Electronics. 2015;**62**(5):3202-3212

[3] Huang W, Abu Qahouq JA. Energy sharing control scheme for state-of-charge balancing of distributed battery energy storage system. IEEE Transactions on Industrial Electronics. 2015;**62**(5):2764-2776

[4] Hu KW, Yi PH, Liaw CM. An EV SRM drive powered by battery/Supercapacitor with G2V and V2H/V2G capabilities. IEEE Transactions on Industrial Electronics. 2015;**62**(8):4714-4727

[5] Shuai L, Corzine KA, Ferdowsi M. Unique ultracapacitor direct integration scheme in multilevel motor drives for large vehicle propulsion. IEEE Transactions on Vehicular Technology. 2007;**56**(4):1506-1515

[6] Dixon JW, Ortuzar ME. Ultracapacitors + DC-DC converters in regenerative braking systems. IEEE Aerospace and Electronic Systems Magazine. 2002;**17**(8):16-21

[7] Delille G, François B. A review of some technical and economic features of energy storage technologies for distribution system integration. Ecological Engineering and Environment Protection. 2009;**1**:40-48

[8] Zhang Z, Zhang X, Chen W, Rasim Y, Salman W, Pan H, Yuan Y, Wang C. A high-efficiency energy regenerative shock absorber using supercapacitors for renewable energy applications in range extended electric vehicle. Applied Energy. 2016;**178**:177-188

[9] Herrera V, Milo A, Gaztañaga H, Etxeberria-Otadui I, Villarreal I, Camblong H. Adaptive energy management strategy and optimal sizing applied on a battery-supercapacitor based tramway. Applied Energy. 2016;**169**:831-845

[10] Ma T, Yang H, Lu L. Development of hybrid battery–supercapacitor energy storage for remote area renewable energy systems. Applied Energy. 2015;**153**:56-62

[11] Abbey C, Joos G. Supercapacitor energy storage for wind energy applications. IEEE Transactions on Industrial Electronics. 2007;**43**(3):769-776

[12] Makhlouf M, Messai F, Benalla H. Modeling and simulation of grid-connected hybrid photovoltaic/battery distributed generation system. Canadian Journal on Electrical and Electronics Engineering. 2012;**3**(1):1-10

[13] Fakham H, Lu D, Francois B. Power control Design of a Battery Charger in a hybrid active PV generator for load-following applications. IEEE Transactions on Industrial Electronics. 2011;**58**(1):85-93

[14] Capasso C, Sepe V, Veneri O, Montanari M, Poletti L. Experimentation with a ZEBRA plus EDLC based hybrid storage system for urban means of transport. In: Proceedings of the 2015 International Conference on Electrical Systems for Aircraft, Railway, Ship Propulsion and Road Vehicles (ESARS); 3-5 March 2015; Aachen, Germany. IEEE; 2015. DOI: 10.1109/ESARS.2015.7101498

[15] Sanfélix J, Messagie M, Omar N, Mierlo JV, Hennige V. Environmental performance of advanced hybrid energy storage systems for electric vehicle applications. Applied Energy. 2015;**137**:925-930

[16] Capasso C, Veneri O, Patalano S. Experimental study on the performance of a ZEBRA battery based propulsion system for urban commercial vehicles. Applied Energy. 2017; **185**(2):2005-2018

[17] Krause A, Kossyrev P, Oljaca M, Passerini S, Winter M, Balducci A. Electrochemical double layer capacitor and lithium-ion capacitor based on carbon black. Journal of Power Sources. 2011;**196**(20):8836-8842

[18] Tan SC, Lai YM, Tse CK, Salamero LM, Wu CK. A fast-response sliding-mode controller for boost-type converters with a wide range of operating conditions. IEEE Transactions on Industrial Electronics. 2007;**54**(6):3276-3286

[19] Wai RJ, Chen MW, Liu YK. Design of adaptive control and fuzzy neural network control for single-stage boost inverter. IEEE Transactions on Industrial Electronics. 2015;**62**(9): 5434-5445

[20] Kolesnikov A. Synergetic control for electromechanical systems. In: Proceedings of the 15th International Symposium on Mathematical Theory of Networks and Systems (MTNS 2002); August 12–16, 2002; University of Notre Dame. 2002

[21] Kondratiev I, Santi E, Dougal R, Veselov G. Synergetic control for m-parallel connected DC-DC Buck converters. In: Proceedings of the 35th Annual IEEE Power Electronics Specialists Conference (PESC 04); 20-25 June 2004; Aachen, Germany: IEEE; 2004. p. 182-188. DOI: 10. 1109/PESC.2004.1355739

[22] Santi E, Monti A, Li D. Synergetic control for power electronics applications: A comparison with the sliding mode approach. Journal of Circuits, Systems, and Computers. 2004; **13**(4):737-760

[23] Guangfu MA, Jing H, Gang L, Chuanjiang L. Adaptive synergetic optimal control for attitude tracking of rigid spacecraft. In: Proceedings of the 30th Chinese Control Conference; July 22–24, 2011; Yantai, China. 2011. p. 1865-1870

[24] Nusawardhana SAK, Crossley W. Nonlinear synergetic optimal control. Journal of Guidance, Control, and Dynamics. 2007;**30**(4):1134-1147

[25] Dhaouadi R, Hori Y, Huang X. Robust control of an ultracapacitor-based hybrid energy storage system for electric vehicles. In: Proceedings of the 13th IEEE International Workshop

on Advanced Motion Control, (AMC2014); March 14-16, 2014; Yokohama, Japan. IEEE; 2014. DOI: 10.1109/AMC.2014.6823275

[26] Buller S, Thele M, De Doncker RWAA, Karden E. Impedance-based simulation models of supercapacitors and Li-ion batteries for power electronic applications. IEEE Transactions on Industry Applications. 2005;**41**(3):742-747

[27] Zubieta L, Bonert R. Characterization of double-layer capacitors for power electronics applications. IEEE Transactions on Industry Applications. 2000;**36**(1):199-205